

DEVELOPMENT OF A STABILIZED WIDEBAND PENDULUM-TYPE GRAVITY DIRECTION SENSOR UTILIZING AN ELECTROMAGNETIC CLUTCH AND BRAKE FOR ANTI-SWING

Tokuji Okada, Akihiro Tsuchida, Tomofumi Mukaiyachi, Toshimi Shimizu

Abstract:

This paper proposes the usefulness of combining an electromagnetic clutch and brake with a pendulum for anti-swing for developing a stabilized wideband pendulum-type gravity direction sensor. The pendulum-type sensor is high in response to direction change but liable to swing even when the change stops, in general. Therefore, anti-swing control without degrading sensitivity of direction measurement is important. Continuous damping of the pendulum motion causes an error in a stationary condition unless the pendulum is free from damping repetitively in an appropriate term. To develop a quick response direction sensor without error, we use a magnetic device. Based on motion analysis of a double pendulum, we simulate behaviours of the pendulum-type sensor by actuating the magnetic device by using different signals in form, frequency and magnitude. Also, we fabricate a motion simulator having two rotation joints to evaluate the anti-swing effect of the magnetic device. In the experiment we demonstrate that the device is beneficial for suppressing pendulum vibration over a wideband for measuring resultant direction of the acceleration compound with motion and gravity on such a platform moving randomly. Also, we show that a triangular signal is better than a sinusoidal signal for making the settling time short; however difference is within a narrow margin.

Keywords: anti-swing, electromagnetic clutch and brake, gravity direction sensor, pendulum, inclinometer.

1. Introduction

Tilt angle is evaluated as an angular displacement from a certain direction. In general, tilt of a plane like a liquid surface or floor is evaluated by two angular values. A sensor of this type is called a *2-axis inclinometer*. In either type, angular displacement is collected by evaluating electric potential using wired, conductive or magneto-resistive resistance, in general. Some other methods paying attention to the liquid level or position of a ball in a cylindrical tube or spherical vessel are reported [1]. A pendulum-type sensor has also been reported so far [2]. This type is sensitive to monitor motion change directly without the affect of offset and hysteresis. On the other hand, it is too delicate to reduce vibration. A servo controlled pendulum sensor can make friction torque zero since a gearing mechanism is not needed for the coupling potentiometer.

Anti-swing techniques for carrying a load by crane have been proposed. In a special edition entitled "What's the essence of the vibration control?", damping material

and new dampers are introduced [3]. There are two types of damping among these. First is the active type that cancels vibration by motors driven by external energy corresponding to the vibration power. Second is the passive type that transforms the vibration power into mechanical or electrical actuation for suppressing vibration without using external energy. At this time, two swing-types having 2 axes and unit-type operating as a vibration absorber are considered as the active type. Actually, some of these are found in MR (Magneto-rheological) dampers [4], anti-sway based on switching in a suitable timing [5], feedback control for a gantry crane [6], use of the gyroscopic stabilising mechanism [7], crane control for anti-swing based on cable roll up or delayed feed back control [8], [9].

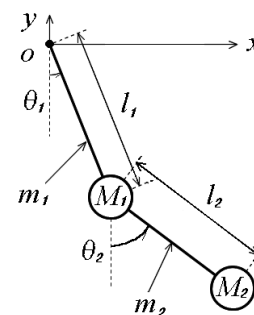


Fig. 1. Definition of parameters for motion analysis of a double pendulum.

As for the passive type, gondola control using a swing damper [3], use of piezoelectric devices [10] are found for instance. In addition, the pendulum mechanism is applied to trains to improve the comfortableness of the ride [11].

This paper describes the development of a stabilized wideband pendulum-type gravity direction sensor utilizing an electromagnetic clutch and brake for anti-swing of a pendulum. We call the electromagnetic clutch and brake *magnetic device* for simplicity. The sensor is intended to stabilize a mobile robot's motion changing its position and acceleration dynamically on irregular terrain. For this purpose, the sensor is needed to measure the direction of resultant acceleration of motion and gravity with simplicity in assembling, signal processing and at reasonable cost. Actually, we propose a pendulum-type gravity sensor that measures the direction of resultant acceleration when the robot moves at high acceleration as an active-type device using the magnetic device instead of a gyroscope. This is because we noticed that a rigid pendulum arm is so sensitive to the robot's change in motion.

We analyze double pendulum motion since this pendulum simulates the measurement environment attaching the sensor to the robot's body while it moves. Simulated results are compared with experimental results to show validity of mathematical equations extracted in the analysis. We clarify the influences of signals in form, frequency and level for actuating the magnetic device to design a high performance pendulum-type gravity sensor.

2. Analysis of a pendulum motion

A. Extraction of mathematical form

Generally, an installed pendulum on a moving object is supposed to be a double pendulum as shown in Fig.1. In the following, we call *first pendulum* for the first rigid arm extending from the rotation centre O , and *second pendulum* for the next rigid arm connected serially to hang a mass which we call *weight* at the end. We analyze motion of the second pendulum in a vertical plane referred by horizontal and vertical axes of X and Y , respectively. Nomenclatures are as follows, where the subscript i stands for the pendulum position, say 1 for the first pendulum for instance.

- g - gravity acceleration
- l_i - length of the pendulum arm
- m_i - mass of the pendulum arm
- M_i - mass of the pendulum weight
- S - settling time of the pendulum
- t - time elapsed
- (x_i, y_i) - mass centre of the pendulum weight
- (X_i, Y_i) - mass centre of the pendulum arm
- θ_i - inclination/rotation angle of the pendulum (CCW from gravity direction is positive)
- ϕ - angle toward which the mass M_2 exists (CCW is positive similarly to θ_i)
- ω - angular velocity of the first pendulum(= $\dot{\theta}_1$)

Let suppose that T_a means total kinetic energy of the mass M_i , then we have

$$T_a = \sum_{i=1}^2 \{M_i(\dot{x}_i^2 + \dot{y}_i^2)/2\} = [(M_1 + M_2)l_1^2\dot{\theta}_1^2 + M_2\{l_2^2\dot{\theta}_2^2 + 2l_1l_2\dot{\theta}_1\dot{\theta}_2 \times \cos(\theta_1 - \theta_2)\}]/2 \quad (1)$$

Also, supposing T_b is total translation energy of the arms, we can write

$$T_b = \sum_{i=1}^2 \{m_i(\dot{X}_i^2 + \dot{Y}_i^2)/2\} = [(m_1 + 4m_2)l_1^2\dot{\theta}_1^2 + m_2\{l_2^2\dot{\theta}_2^2 + 4l_1l_2\dot{\theta}_1\dot{\theta}_2 \times \cos(\theta_1 - \theta_2)\}]/8 \quad (2)$$

Assuming that the two pendulum arms are composed of uniform material yields total arm rotation energy T_q .

$$T_q = \sum_{i=1}^2 \{m_i l_i^2 \dot{\theta}_i^2 / 24\} \quad (3)$$

Concerned with potential energy expressed as V , it follows that

$$\begin{aligned} V &= gM_1(l_1 + y_1) + gM_2(l_1 + l_2 + y_2) + \quad (4) \\ &+ gm_1(l_1/2 + Y_1) + gm_2(l_1 + l_2/2 + Y_2) \\ &= gl_1(1 - \cos \theta_1)(M_1 + M_2 + m_1/2 + m_2) + \\ &+ gl_2(1 - \cos \theta_2)(M_2 + m_2/2) \end{aligned}$$

All of these energies are summed up to have L

$$\begin{aligned} L &= T_a + T_b + T_q - V \quad (5) \\ &= A_1\dot{\theta}_1^2 + A_2\dot{\theta}_2^2 + A_3\dot{\theta}_1\dot{\theta}_2 \cos(\theta_1 - \theta_2) - \\ &- A_4(1 - \cos \theta_1) - A_5(1 - \cos \theta_2), \end{aligned}$$

where

$$A_1 = l_1^2 (3M_1 + 3M_2 + m_1 + 3m_2)/6 \quad (6)$$

$$A_2 = l_2^2 (3M_1 + m_2)/6 \quad (7)$$

$$A_3 = l_1 l_2 (M_2 + m_2/2) \quad (8)$$

$$A_4 = gl_1 (M_1 + M_2 + m_1/2 + m_2) \quad (9)$$

$$A_5 = gl_2 (M_2 + m_2/2) \quad (10)$$

At this moment, introducing a root rotation of the first pendulum with a constant angular velocity makes ω constant. Substituting Eq. (5) into the Lagrange's equation results in the form [12].

$$2A_2\ddot{\theta}_2 + c\dot{\theta}_2 + A_5 \sin \theta_2 - A_3\omega^2 \sin(\theta_1 - \theta_2) = 0, \quad (11)$$

where c means a resistance coefficient under the case where resistive force occurs proportionally to the second pendulum's angular velocity. When the mass M_2 , called weight afterwards simply falls freely from the angle ϕ [rad], ω becomes zero. Therefore,

$$2A_2\ddot{\theta}_2 + c\dot{\theta}_2 + A_5 \sin \theta_2 = 0 \quad (12)$$

Unknown parameters θ_2 in Eqs. (11) and (12) are solved by the Runge-Kutta method for instance.

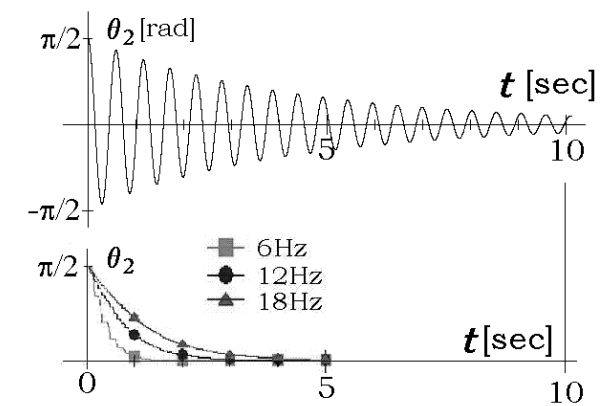


Fig. 2. Swing angles in the upper and lower parts depend on the condition when the clutch/brake is activated or not in the case when ω takes zero and the mass M_2 falls freely from $\phi = -\pi/2$ [rad].

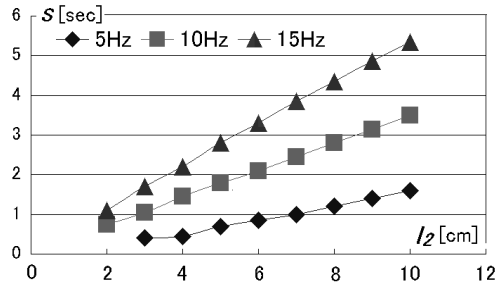


Fig. 3. Analytical settling time versus l_2 when the pendulum falls freely from $\phi = -\pi/2$ [rad].

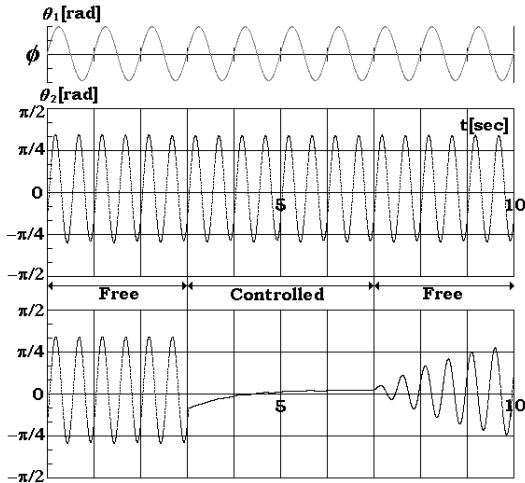


Fig. 4. Analytical results of the characteristics of θ_2 versus t when the pendulum l_2 swings $\pm\pi/3$ [rad] around the direction of $\phi = -\pi/2$ [rad].

B. Simulation of pendulum motion using numerical method

B.1. In the case when pendulum root is immovable

We estimate pendulum motion by solving θ_2 of the differential equation Eq. (12). Actually, suppose that the weight falls from a lateral direction ($\phi = -\pi/2$ [rad]) under such that $l_1 = 13.1$ [cm], $l_2 = 7$ [cm], $m_1 = M_1 = 0$, $m_2 = 6.86 \times 10^{-2}$ [N], and $M_2 = 1.568 \times 10^{-1}$ [N]. Then characteristics of θ_2 versus t are shown in the upper part of Fig.2. Under the same conditions, we regulated the pendulum root by applying a brake-on and brake-off signal repetitively, i.e. lock and release, called intermittent signal, to the numerical method for locking the root with a duty ratio 0.5 and evaluated the settling time of the pendulum. Our settling time is defined as the time required making the pendulum stable within a permissible error of $\pm\pi/180$ [rad]. Lower part of the figure shows the results when the signal has frequencies of 6, 12, and 18 [Hz]. From the figure we can confirm that the frequency 6[Hz] makes the time shorter in most cases.

Settling time is also affected by pendulum length l_2 . The time using the intermittent signal of frequencies 5, 10, and 15 [Hz] is shown in Fig.3. These results imply that the settling time becomes shorter when the frequency is lower and the length is shorter.

B.2. In the case when pendulum root swings

Suppose that the first pendulum root is activated

to swing $\pm\pi/3$ [rad] from the datum direction $\phi = -\pi/2$ [rad], its motion is simulated and shown in Fig.4 under such conditions that $l_2 = 6$ [cm], $m_2 = 5.88 \times 10^{-2}$ [N], $M_2 = 1.568 \times 10^{-1}$ [N], and swing frequency 1 [Hz]. The upper and middle parts are the results of θ_1 and θ_2 , respectively. From these we notice that the second pendulum swings two times in one cycle swing of the first pendulum. The lower part shows the motion of the second pendulum when the second pendulum root is regulated from the vertical base by an intermittent signal in the period when the time elapses from 3 to 7 seconds under the same conditions mentioned before.

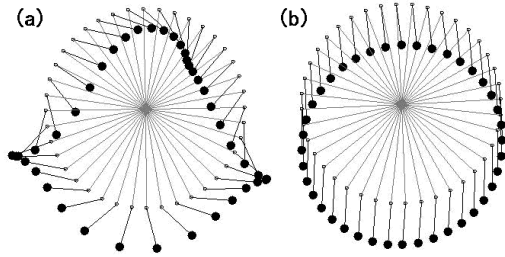


Fig. 5. Comparison of a simulated pendulum motion with and without anti-swing when the motion pendulum root rotates at a constant speed 60[rpm] under $l_2 = 5.4$ [cm].

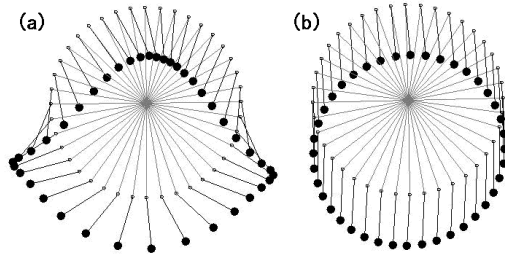


Fig. 6. Comparison of a simulated pendulum with and without anti-swing when the pendulum root rotates at a constant speed under $l_2 = 7.0$ [cm].

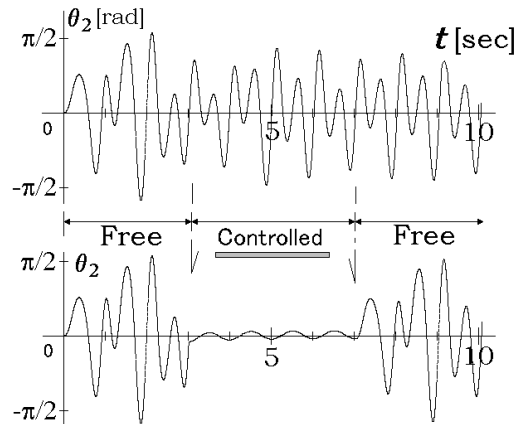


Fig. 7. Simulated motion of the double pendulum when ω is constant. Swing angles of θ_2 are shown in free and controlled conditions at the upper and lower parts, respectively.

B.3. In the case when the pendulum root rotates at a constant speed

A double pendulum is formed when the arm l_1 rotates at a constant speed. And the weight has a tendency to face in the direction of the resultant acceleration of θ_2 versus t , weight position is collected by changing θ_1 with an increment of $\pi/20$ [rad], and displayed by black circles

in Fig. 5(a). Rotation is considered under the condition such that $l_1=13.1$ [cm], $l_2=5.4$ [cm], $m_1=M_1=0$, $m_2=5.292 \times 10^{-2}$ [N], $M_2=1.568 \times 10^{-1}$ [N] and $\omega=2\pi$ [rad/s] (=60 [rpm]) in CCW. In such a case when $l_2=7.0$ [cm] and $m_2=6.86 \times 10^{-2}$ [N], we have the results found in Fig. 6(a). From these figures, it is evident that the weight direction is greatly affected by the root rotation. And it is confirmed that the direction is dependent on the amount of ω .

On the other hand, the direction change of the weight is stabilized when the second pendulum root is regulated by the intermittent signal of 18 [Hz]. Actually, calculated results of the previous rotation are shown in Fig. 5(b) and Fig. 6(b). One can observe that the pendulum swing is drastically suppressed to prove the anti-swing effect.

Similar conditions to get the results shown in Fig. 6 are applied to calculate θ_2 versus t characteristics shown in Fig. 7. The period from $t=3$ [s] to 7 [s] in the lower part of the figure shows the regulated results from the vertical base by the intermittent signal of 18 [Hz]. From this figure, we can confirm that the pendulum swing decreases sharply to pursue the anti-swing effect.

3. Fabrication of sensor and swing generator

In order to certify the anti-swing effect quantitatively, it is necessary to develop an appropriate pendulum-type gravity direction sensor. Also, it is beneficial to devise a simple electro-mechanical generator producing a variety of vibration. Fabrication of these is described in the following.

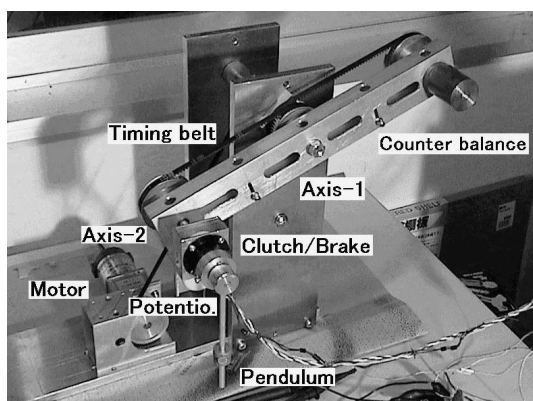


Fig. 8. Outlook of the fabricated experimental set.

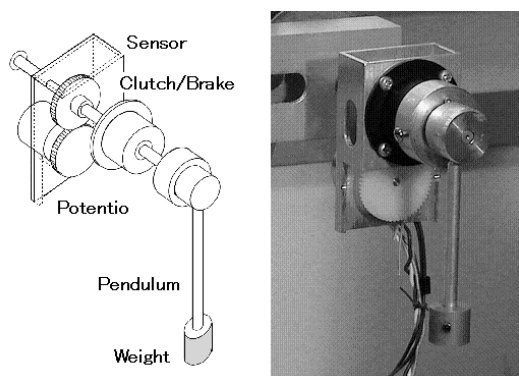


Fig. 9. Gravity sensor combined with the electro-magnetic clutch and brake.

A. Construction of gravity direction sensor

There is an overview of the experimental set in Fig. 8. Main components of the set are a pendulum-type gravity sensor and vibration generator on which the sensor is attached. The sensor is assembled by combining a pendulum with a magnetic device coaxially, and also with a potentiometer by a gearing mechanism. Actually, the clutch and brake of a diameter of 28 [mm] and thickness of 14 [mm] (Miki pulley AP05Y07), and potentiometer (Midorisokki CP-3M) are assembled to measure the angle θ_2 (see Fig. 9). The pendulum root is suspended on the rectangular frame through radial bearings. This root fixes a pendulum arm and guides a thin elastic disc of the magnetic device so that it can slide toward the axial direction freely.

On the other hand, the device has coils fixed to the rectangular frame and attracts the disc with proportional force to electric current flowing through the coils. Therefore, the pendulum is free to move when no current flows. That is, the pendulum motion is regulated easily by an appropriate current so that the attractive force is controlled analogously from zero to a certain value. With a large force, the pendulum is locked from instantaneous rotation.

B. Preparation of a vibration generator

When the sensor is attached to a moving object, the sensor weight has a tendency to find a relaxed direction by rotating for pointing resultant direction of gravity and motion. The tendency has the advantage of controlling the table so that it can keep a vessel steady without spilling the liquid contents. When the sensor is attached to a slow motion robot, the direction is assumed as the gravity direction and is useful for controlling platforms for loading or seating horizontally on an irregular terrain. Basically, the principal aim of the sensor is to measure angular shift quantitatively from gravity direction even when the sensor is attached on an object moving with high acceleration in 3-D space. However, in our leg-type locomotion environment, the sensor should measure robot posture in the sagittal plane (pitch) or coronal plane (roll) without the affect of vertical swing. Evidently, sudden change of motion disturbs the measurement.

Principally, the sensor is composed of a pendulum having a single arm. And the pendulum root moves in a real measurement environment on a mobile robot. This is the reason why the double pendulum is discussed in section 2.A. This idea initiated us to fabricate a vertical vibration generator. This is overviewed like a gondola (Ferris wheel) since it has a rotating wheel around a horizontal axis and hangs a weight from the wheel rim pivot. The platform for carrying spectators is assumed to be a pendulum hanging from the weight. The hanged object is counter-balanced.

The wheel centre axis is driven by a DC motor (SS23F-LH50 24V) with reduction gear(1/50). According to the motor input signal, the first pendulum root can rotate CW and CCW. Also, it can swing around an assigned direction within a limited range. Original signals are produced by a signal generator (Iwatsu SG-4101). Amplified signals having a sinusoidal, triangular or rectangular form serve to drive the motor.

C. Sensor installation on the vibration generator

Since the pendulum root is freely supported by radial bearing at the rim, the gearing mechanism of the potentiometer gives angular displacement of the pendulum arm from a certain angle on the rim body. Therefore, it is necessary to integrate angles of wheel rotation and potentiometer output to extract angular displacement of the arm from gravity direction, said to be the inclination angle. But this integration is time consuming and not good for real time measurement. To measure the inclination angle in real time, we propose the use of an immovable base as a part of the ground at the pivot joint because the base gives the angular index for understanding potentiometer output. In fact, we generated the base by connecting two same sized sprockets with a timing belt. One sprocket is fixed to the vibrator body located at the wheel centre. The other sprocket is attached to the cylinder supported at the pivot joint. The timing belt (Bridgestone S3M414) is efficient to generate the base at the joint (see Fig.8).

The base having a cylindrical form is attached to the aforementioned rectangular tube on which the potentiometer is attached. Since the second pendulum root is free to rotate coaxially on the cylinder, potentiometer output means the exact data of our measurement. That is, the rectangular tube always keeps the same posture regardless of wheel rotation.

A variety of robot vibration is produced at the pivot joint by transferring a variety of signals to a motor. At the same time the potentiometer can measure the inclination angle of the pendulum without disturbance. Therefore, the assembly is beneficial to collect data effectively and to evaluate swing suppression ability of the magnetic device directly without calculation even when a full-scaled robot is not available.

4. Experimental results

To certify the anti-swing effect of the magnetic device, pendulum motion is observed while its root swings or rotates, in addition to free fall of the weight from a fixed position even when the pendulum root remains at the same position.

A. Driving signal of the magnetic device

An appropriate amount of damping is needed to suppress pendulum vibration but it must be released at a certain interval to avoid steady error even when there is no vibration. Unfortunately, there is no way to determine release timing and interval for adapting to unknown vibration at this moment. Also, the damping should be gentle so that there is no shock to the pendulum. This implies that a pulse form signal is not good for driving the magnetic device; however we used the form as an intermittent signal in the simulation for calculation simplicity.

We noticed that a repetitive signal like a sinusoidal wave is useful. However, the device produces an attractive force regardless of signal sign. This operation looks as if a full-wave rectified signal is inputted. Therefore, relaxing time generated by this plus and minus repetitive signal is momentary and not enough to track motion correctly. Our solution is to assign an equal interval to

produce brake force and relaxing time. To apply this, we used a modified repetitive signal based on half-wave rectification. This rectification is easily performed by inserting a diode in the electric circuit for driving the device. The time interval is controlled by changing the frequency of an original signal. Actually, the positive part of a signal from the function generator (Iwatsu FG-330) is rectified for producing a smooth brake force. Its negative part makes the brake force zero.

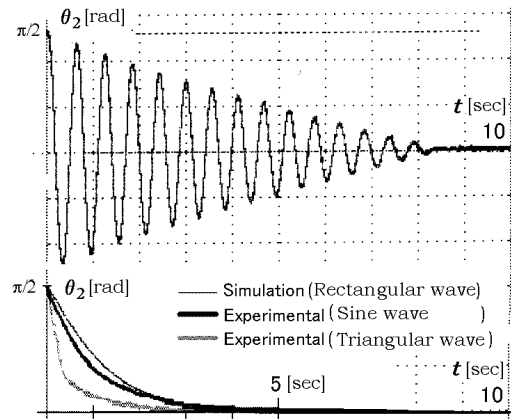


Fig.10. Experimental characteristics of θ_2 versus t when the weight falls freely from $\phi = -\pi/2$ [rad]. Analytical and experimental results are in the upper and lower parts, respectively.

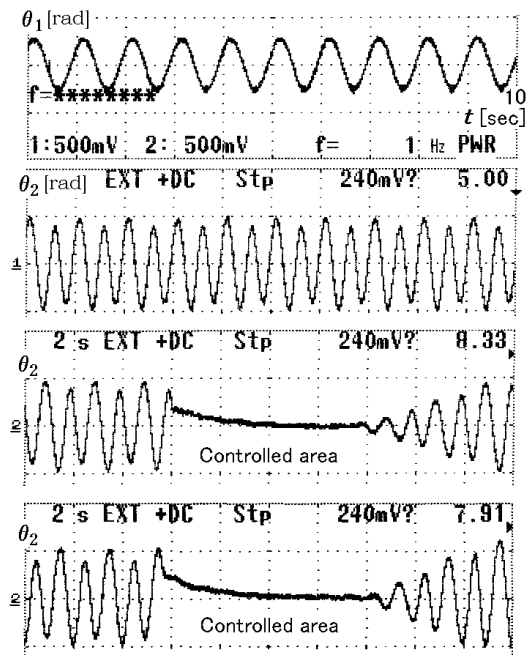


Fig.11 Experimental characteristics of θ_2 versus t when the weight swings $\pm\pi/3$ [rad] from the datum direction $\phi = -\pi/2$ [rad].

B. Free fall of the weight

In the case when the pendulum root is immovable in the direction $\theta_1 = -\pi/3$ [rad], we released the weight from the direction of $\phi = -\pi/2$ [rad] so that it falls freely. Its behaviour is observed for comparing motion with and without the brake force.

Other motion is demonstrated by changing the signal in form, frequency and arm length. A storagescope (Iwatsu DS-8710) collected so much data easily. The upper

part of Fig. 10 shows memorized wave forms concerned with θ_2 versus t under $\phi = -\pi/2$ [rad]. The lower part compares difference of θ_2 versus t when the magnetic device is driven by signals of pulsating, sinusoidal and triangular form for half-wave rectification. In the figure, a frequency of 6[Hz] has been proven to be better in Fig. 2. Evidently, pendulum swing is remarkably suppressed in each of the three signals. Triangular form is rather good in the three.

C. In the case when pendulum root swings

From the results shown in section 2.B, it is supposed that ϕ influences the generation of many types of vibration. Obviously, one can say that the vibration becomes larger in the vicinity of $\phi = \pi/2, \pi, \text{ and } 3\pi/2$ [rad]. This is clearly observed in our experiment. To show one example of this, let's suppose that swing frequency 1[Hz], half-wave rectified sinusoidal and triangular form of frequency 18[Hz], and $\phi = -\pi/2$ [rad], $-\pi/3 < \theta_2$ [rad] $< \pi/3$, $l_2 = 6$ [cm], $m_2 = 5.88 \times 10^{-2}$ [N], $M_2 = 1.568 \times 10^{-1}$ [N]. Then, time dependent pendulum motion is monitored by the storagescope (See Fig.11). The first and second parts in the upper area show θ_1 and θ_2 when there is no brake force, respectively.

The first and second parts in the lower area show θ_2 when the signal to the magnetic device has half-wave rectified sinusoidal and triangular forms, respectively. Brake force is given in the period from $t = 3$ to $t = 4$. These results confirmed that the brake force prevents the arm from excessive swing. In addition, the triangular form is superior to the sinusoidal form; however difference is within a narrow margin. Also, it is confirmed that wave forms of θ_2 are deformed from those obtained in the simulation (see Fig. 4). These might be caused by the fact that ω drifts since θ_1 is simply changed by a feed forward control without thinking about load difference between move-up rotation and move-down rotation. Other factors are pointed out in low motor response to control θ_1 because motor inertia and reduction gear ratio are not considered. However, it is true that the vibration caused by the pendulum root swing is drastically suppressed.

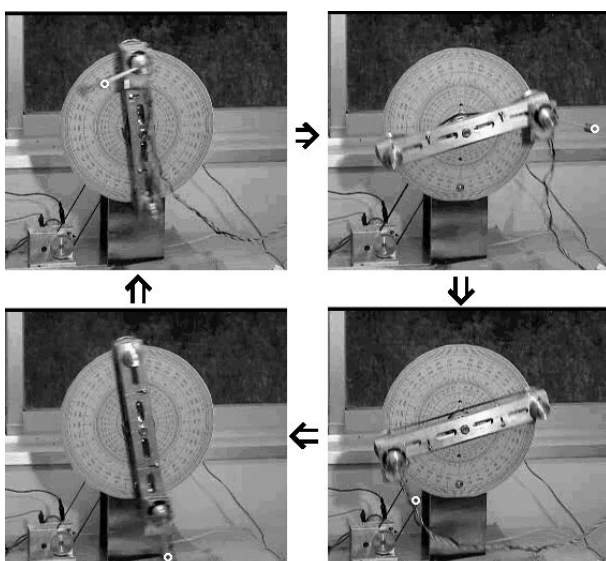


Fig. 12. Pendulum direction when the magnetic device is inactive for free rotation.

D. In the case when pendulum root rotates

In the experiment of irregular pendulum root rotation, the brake force operates effectively also to suppress pendulum vibration. However, the pendulum behaves different with the affect of a small angular error of arm direction in the initial state of rotation, and becomes chaotic to form different motion patterns.[12]. These motions are not shown because of the limited number of pages. Hori [13] verified the possibility of controlling this motion with stability by the method called OGY. In this paper, we show experimental results performed under the same conditions that were used to get the results in Figs. 6 and 7. However, the driving signal was changed from the intermittent to triangular forms, and the first pendulum rotates CW under such conditions that $l_2 = 3$ [cm], $m_2 = 2.94 \times 10^{-1}$ [N], and $M_2 = 9.8 \times 10^{-1}$ [N]. Figs.12 and 13 show results without and with brake force, respectively. In these figures, weight positions are marked with white circles for ease of understanding θ_2 . The front circular board is a big protractor to help in measuring θ_1 with the naked eye.

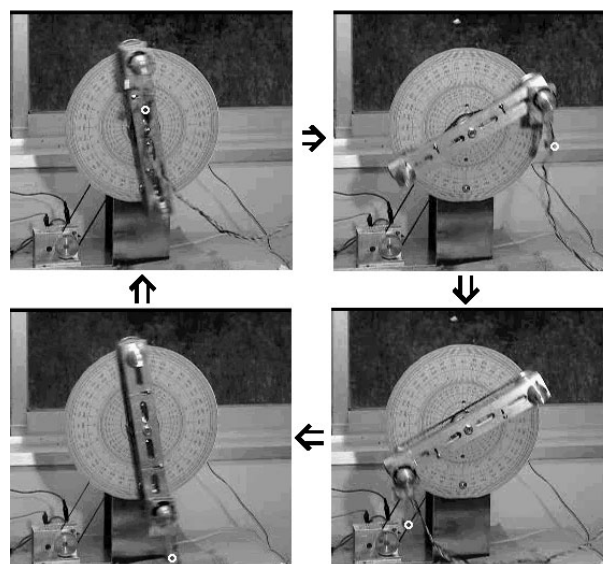


Fig. 13. Pendulum direction when the magnetic device is activated for anti-swing.

Fig. 14 shows the collected wave form of θ_2 in the demonstration shown in Fig. 13 using signals of half-wave rectified sinusoidal and triangular forms. Brake force is not applied in the upper part, but applied in the middle and lower parts using the triangular form and sinusoidal forms, respectively. Advantages of the brake force are also verified here. Triangular form is superior to the sinusoidal form; however the difference is within a narrow margin.

Magnitude of the driving signal in the aforementioned three cases has not been discussed so far; however fundamental experiments proved that the brake force increases as much electric current flows through the device. These preparatory experiments helped us to find the appropriate voltage that is determined by considering input impedance of the device.

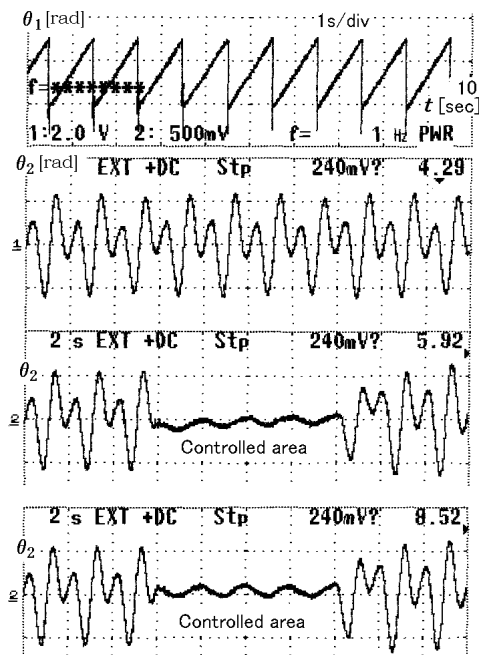


Fig. 14. Experimental motion of the double pendulum motion when $\dot{\theta}_1$ is constant. Swing angles of θ_2 are shown at the upper and lower parts depending on inactive and active controls of the magnetic device, respectively.

5. Concluding remarks

We proposed the construction of a pendulum-type gravity direction sensor using a potentiometer combined with a magnetic device. Also, we showed the design of the sensor with a vibration generator for evaluating sensor performance. In this paper, the magnetic device is fixed on the first arm but on the vertical base to avoid cable twist when the first arm rotates. In the simulation of sensing the gravity direction, we calculated the inclination angle of the pendulum arm and also verified that the calculated results became similar to those observed in a practical demonstration.

In the experiment giving brake force to a pendulum root, we proved that the force was valuable to suppress pendulum vibration from both analytical and experimental considerations. Particularly, a signal of half-wave rectified sinusoidal form has the advantage of driving the device for making settling time short. The signal of a half-wave rectified triangular form was effective in its anti-swing performance; however the difference was so small. For making the settling time short we confirmed from the experiment that a pendulum having a short and long arm was valid for narrow and wide band vibration, respectively.

Since the proposed pendulum-type sensor could measure gravity direction angle without the affect of vibration, its output might be utilized to control a robot seat for comfortable riding, for instance. Application into a servo loop will always keep the seat horizontal and guide normal equilibrium sense to a driver.

The magnetic device was so small in size and power for suppressing vibration. The powered-up device will serve not only as a sensor but also as an actuator to suppress swing of a crane, for instance. To improve sensor performance for anti-swing and powered-up use as an actuator, it is worth while to determine signal frequency and duty

ratio by considering inertial moment of the pendulum arm and weight. The proposed sensor will be helpful as a 3-D pendulum-type gravity sensor by supporting the pendulum root in a spherical joint. These subjects are part of our plan for the future.

AUTHORS

Tokuji Okada* and **Tomofumi Mukaiyachi** - Niigata University, Department of Biocybernetics, Ikarashi 2-8050, Niigata-Shi, Japan 950-2181. E-mail: okada@eng.niigata-u.ac.jp.

Akihiro Tsuchida and **Toshimi Shimizu** - Graduate School of Niigata University, Ikarashi 2-8050, Niigata-Shi, Japan 950-2181.

* Corresponding author

References

- [1] T. Okada, K. Kurosaki, K. Berns, R. Dillmann, "Measurement of resultant acceleration in 3D space based on sensing a metallic ball position on elastic layer located at inside of a spherical vessel", *Trans. of SICE*, no. 787/796, 2005, pp. 41-10.
- [2] Daniel Inaudi, Branko Glisic, "Development of a fiber-optic interferometric inclinometer". In: *Proc. SPIE Int. Symp. on Smart Structure and Materials*, no. 4694, 2002, pp. 36-42.
- [3] K. Suzuki, "Damping and passive vibration control-Development of damping material and new dampers-", *J. of SICE*, no. 37-8, 1998, pp. 531-540.
- [4] C. Sakai, T. Terasawa, A. Sano, "Adaptive identification of MR damper with application to vibration control", *Trans. SICE*, vol. 42, no. 10, 2006, pp. 1117-1125.
- [5] R. Kondo, S. Shimahara, "Anti-sway control of a rotary crane via two-mode switching control", *Trans. SICE*, vol. 41, no. 4, 2005, pp. 307-313.
- [6] Yannick Aoustin, Alexander Formal'sky, "Simple anti-swing feedback control for a gantry crane", *Robotica*, vol. 21, 2003, pp. 655-666.
- [7] O. Nishihara, H. Matsushita, S. Sato, "Vibration damping mechanisms with gyroscopic moments", *Trans. JSME*, vol. 57C-534, 1991, pp. 497-503.
- [8] Ho-Hoon Lee, "A new approach for the anti-swing control of overhead cranes with high speed load hoisting", *Int. J. of Control*, vol. 76, no. 15, 2003, pp. 1493-1499.
- [9] Ziyad N. Masoud, Alih. Nayfeh, Nader A. Nayfeh, "Sway reduction on quay-side container cranes using delayed feedback controller: Simulations and experiments", *J. of Vibration and Control*, vol. 11, no. 8, 2005, pp. 1103-1122.
- [10] T. Fujita, H. Nomura, M. Yasuda, A. Matsuura, M. Tsuchiya, "Fundamental study of passive microvibration control with smart structure using piezoelectric devices", *Trans. JSME*, vol. 66C-644, 2000, pp. 1097-1101.
- [11] *Technical report of Kawasaki Heavy Industry*, Special edition on railway wagon, no. 160, 2004.
- [12] M. Komuro, "Double pendulum and chaos", *J. of RSJ*, vol. 15, no. 8, 1997, pp. 1104-1109.
- [13] H. Shikano, Y. Hori, "Stabilizing control of double pendulum using reconstructed attractor", *Trans. IEE Japan*, vol. 120D-1, 2000, pp. 142-147.